ACCSCIENCE PUBLISHING

Tumor Discovery

ORIGINAL RESEARCH ARTICLE

Identification of *BAK1* as a novel prognostic biomarker for liver cancer based on the mining of liver cancer pyroptosis-related genes

Yiyang Chen[1], Wanbang Zhou[2], Yiju Gong[2], and Xi Ou[1]*

[1]Anhui Medical University, Clinical College of Peking University Shenzhen Hospital, Fifth Clinical Medical College of Anhui Medical University, China

[2]Peking University Shenzhen Hospital Clinical School, Futian District, Shenzhen, Guangdong Province, China

Abstract

Hepatocellular carcinoma is a type of digestive tract cancer that has a high incidence and a poor prognosis. Pyroptosis, a newly discovered and proven method of pro-inflammatory programmed cell death, is linked to tumor development, patient prognosis, and response to therapy. In this study, the prognostic genes of liver cancer were obtained; their expressions were extracted from The Cancer Genome Atlas database; differential analysis, survival analysis, and clinical correlation analysis were performed; and a nomogram was constructed to predict the survival rate. Based on the expression of *BAK1* gene, all samples were then divided into two groups: High expression and low expression. Enrichment analysis, immunological analysis, and drug susceptibility analysis of differential genes were subsequently performed in that order. *BAK1* expression was found to be significantly higher in liver hepatocellular carcinoma (LIHC). High *BAK1* expression levels were found to be linked to cancer development and poor prognosis. To assess the diagnostic value of *BAK1* in LIHC, a receiver operating characteristic curve was drawn. In addition, there were significant differences in drug sensitivity between high and low *BAK1* expression in 90 drugs. The *BAK1* gene may be a good potential LIHC diagnostic marker, an oncogene in the occurrence and progression of liver cancer, a new prognostic biomarker, and a potential therapeutic target for liver cancer.

Keywords: *BAK1*; Liver cancer; Pan-cancer; Immunity; Biomarkers; Prognosis

***Corresponding author:**
Xi Ou
(bdszyyox@163.com)

Citation: Chen Y, Zhou W, Gong Y, *et al*., 2022, Identification of *BAK1* as a novel prognostic biomarker for liver cancer based on the mining of liver cancer pyroptosis-related genes. *Tumor Discov,* 1(2): 221. https://doi.org/10.36922/td.v1i2.221

Received: October 13, 2022
Accepted: November 15, 2022
Published Online: December 8, 2022

Copyright: © 2022 Author(s). This is an Open Access article distributed under the terms of the Creative Commons Attribution License, permitting distribution, and reproduction in any medium, provided the original work is properly cited.

Publisher's Note: AccScience Publishing remains neutral with regard to jurisdictional claims in published maps and institutional affiliations.

1. Introduction

Hepatocellular carcinoma is a type of digestive tract cancer that has a high incidence and a poor prognosis. In recent years, the survival rate of liver cancer has improved due to the use of surgical resection as the primary treatment method and the development of immunotherapy[1]. Despite continuous advancements in medical technology, in the face of rising incidence, it is difficult to detect liver cancer in the early stages, and once it occurs, it metastasizes easily and has a poor prognosis[2]. Liver cancer is also one of the leading causes of cancer-related death, and the overall 5-year survival rate for patients with liver cancer remains <15%[3,4]. Therefore, novel diagnostic markers for liver cancer are urgently needed to improve the present therapeutic environment for liver cancer. Pyroptosis is a

newly discovered and proven method of programmed cell death with pro-inflammatory characteristics. It is classified into caspase-1-dependent classical pyroptotic pathway and caspase-4/5/11-dependent non-classical pyroptotic pathway. Pyroptosis is characterized by deoxyribonucleic acid (DNA) breakage, cell membrane rupture, and the release of pro-inflammatory proteins[5,6]. According to research, the expression of caspase-1 is low in liver cancer tissue[7]. Other research has demonstrated that hypoxia-induced caspase-1 activation and the subsequent generation of different inflammatory factors in liver cancer tissues and cell lines can promote cancer cell invasion and metastasis[8]. Pyroptosis not only impedes tumor cell proliferation but also creates a microenvironment that promotes tumor cell development[9,10]. Given the importance of pyroptosis in malignancies, the aim of this work was to identify HCC pyroptosis-related genes (PRGs) and investigate their implications in HCC prognosis.

To identify prognosis-related pyroptosis genes, the prognostic value of 52 PRGs in 115 HCC patients from the Gene Expression Omnibus (GEO, GSE 76427) cohort was examined. Following the selection of *BAK1* target gene, its expression level was obtained from The Cancer Genome Atlas (TCGA) database. In addition to the construction of a nomogram, differential analysis, survival analysis, and clinical correlation analysis were carried out to predict the survival rate. Subsequently, all samples were separated into two groups based on *BAK1* gene expression: High and low expression. Enrichment analysis, immunological analysis, and drug sensitivity analysis were performed on the differential genes. The role of *BAK1* in predicting prognosis and immunotherapy response in patients with liver cancer was investigated.

2. Materials and method

2.1. Data sources

The clinically relevant data and gene expression of liver cancer were downloaded from TCGA database (https://portal.gdc.cancer.gov/). The GEO (https://www.ncbi.nlm.nih.gov/geo/) was also used in this work. For the following analysis, a GEO HCC cohort (GSE 76427) and a TCGA cohort were collected. Thereafter, the transcriptome and clinical data were combined and ID transformed. Fifty-two pyroptosis-related genes (REACTOME PYROPTOSIS) were obtained from previously published studies and the Molecular Signatures Database (MSigDB) (http://www.broad.mit.edu/gsea/msigdb/)[11,12]. TCGA and GEO data were integrated in R studio using "limma" and "sva" packages, and the expression of the PRGs was retrieved from the merged data. Finally, the survival analysis of pyroptotic genes was performed to obtain the prognosis-related pyroptotic genes.

2.2. Gene expression and survival prognostic analysis

Using the "Diff Exp" module on the Tumor Immunity Estimation Resource (TIMER) website (http://timer.cistrome.org/) and the R studio software, we investigated *BAK1* expression in 33 human tumor and normal control tissues from the TCGA database. In LIHC, the packages "limma," "ggplot2," and "ggpubr" performed differential and pairwise differential analyses on *BAK1*. Kaplan–Meier curves created by the R studio programs "survival" and "survminer" were used to analyze the differences in survival between subtypes. Univariate and multivariate independent prognostic analyses were then carried out to determine if *BAK1* could be used independently of other prognostic indicators.

2.3. Clinical correlation analysis and coexpression analysis

Clinical correlation analyses and heatmaps were created in R studio using "limma," "ComplexHeatmap," and "ggpubr" packages. Genes that share the same promoter as *BAK1* were identified. A correlation coefficient larger than zero between the two indicates that the gene is positively regulated by *BAK1*, while a correlation coefficient lesser than zero indicates that the gene has a negative regulatory interaction with *BAK1*. The filter condition of the coefficient of correlation was corFilter = 0.6; the filter condition of the correlation test *P*-value was pFilter = 0.001, and the coexpression circle graph was drawn based on the coexpression results.

2.3. Gene enrichment analysis

The samples were separated into two groups with high and low *BAK1* expression levels, respectively, using "limma" and "pheatmap" packages in R studio. A gene heat map with differences between the high and low expression groups was generated. The logFCfilter parameter was set to 1, the fdr filter condition was fdrFilter = 0.05, and the adjusted *P*-value was 0.05. We performed Kyoto Encyclopedia of Genes and Genomes (KEGG) analysis of differential genes in R studio program using "org.Hs.eg.db," "clusterprofiler," and "enrichplot" packages to further investigate the enrichment of probable pathways of differential genes in different groups. To further explore the enrichment of potential pathways of differential genes in different groups, we performed KEGG and GSEA enrichment analysis.

2.4. Immune correlation analysis and drug sensitivity analysis

Through differential analysis of immune cells, immune cells with statistical significance between high and low *BAK1* expression groups were discovered, and differential analysis

was performed on them. To assess the relationship between high and low *BAK1* expression groups and immune cell infiltration content, the CIBERSORT algorithm was used, and the filter condition for immune cell infiltration findings was set to pFilter = 0.05. Immune checkpoint correlation analysis was then performed to investigate the relationship between immune checkpoint genes and *BAK1*, with the filter condition of correlation test *P*-value set to pFilter = 0.001. The immunoscores of liver cancer patients were gathered from http://tcia.at/, and immunotherapy analysis was performed in R studio program using "limma" and "ggpubr" packages. The immunohistochemical pictures of BAK1 protein in various cancer and normal tissues were obtained from http://www.proteinatlas.org/(Human Protein Atlas [HPA] database). We estimated the half maximal inhibitory concentrations (IC50s) of compounds collected from the Genomics of Drug Sensitivity in Cancer (GDSC) website in the TCGA project of the LIHC dataset to identify possible medications for clinical application in LIHC therapy. The IC50 of the chemical, acquired from the GDSC website, in LIHC patients was predicted using R studio's "pRRophetic" package, with the filter condition for *P*-value set to pFilter = 0.001.

2.5. Building a nomogram scoring system

The clinical variables and risk scores were integrated to construct a predictive nomogram in R studio using "rms," "survival," and "regplot" packages. Each clinical feature and risk rating in the nomogram was assigned a score; the total score was calculated by summing the scores for all clinical features and risk ratings in each sample. The accuracy of anticipated 1-, 3-, and 5-year survival events was described using calibration plots.

2.6. Statistical analysis

R version 4 was used for all statistical studies. Statistical significance was defined as $P < 0.05$.

3. Results

3.1. Expression and survival analysis of BAK1

Table 1 lists the 33 cancers studied in this work. The HCC cohort (GSE76427) used has 115 patients in total. We analyzed the PRGs in 115 HCC patients using R studio packages "survival" and "limma." $P < 0.05$ was deemed statistically significant for prognosis. Figure 1A depicts the gene coexpression relationship, revealing that *GSDME*, *CHMP4B*, *CHMP3*, *BAK1*, and *NOD2* are high-risk genes that are strongly associated with prognosis. In view of the limited number of research on the prognosis and immunity of *BAK1* expression in liver cancer, we chose *BAK1* and used TIMER 2.0 database to investigate *BAK1* expression in pan-cancer. Figure 1B shows that the expression of *BAK1* was significantly upregulated in 11 cancer types (bladder urothelial carcinoma [BLCA], breast invasive carcinoma [BRCA], cholangiocarcinoma [CHOL], esophageal carcinoma [ESCA], glioblastoma multiforme [GBM], head-and-neck squamous cell carcinoma [HNSC], liver hepatocellular carcinoma [LIHC], lung adenocarcinoma [LUAD], lung squamous cell carcinoma [LUSC], stomach adenocarcinoma [STAD], and uterine corpus endometrial carcinoma [UCEC]; all $P < 0.001$), whereas it was

Table 1. 33 cancer types used in this study

Abbreviation	Full name
ACC	Adrenocortical carcinoma
BLCA	Bladder urothelial carcinoma
BRCA	Breast invasive carcinoma
CESC	Cervical squamous cell carcinoma and endocervical adenocarcinoma
CHOL	Cholangiocarcinoma
COAD	Colon adenocarcinoma
DLBC	Lymphoid neoplasm diffuse large B-cell
ESCA	Esophageal carcinoma
GBM	Glioblastoma multiforme
HNSC	Head and neck squamous cell carcinoma
KICH	Kidney chromophobe
KIRC	Kidney renal clear cell carcinoma
KIRP	Kidney renal papillary cell carcinoma
LAML	Acute myeloid leukemia
LGG	Low grade glioma
LIHC	Liver hepatocellular carcinoma
LUAD	Lung adenocarcinoma
LUSC	Lung squamous cell carcinoma
MESO	Mesothelioma
OV	Ovarian serous cystadenocarcinoma
PAAD	Pancreatic adenocarcinoma
PCPG	Pheochromocytoma and paraganglioma
PRAD	Prostate adenocarcinoma
PEAD	Rectum adenocarcinoma
SARC	Sarcoma
SKCM	Skin cutaneous melanoma
STAD	Stomach adenocarcinoma
TGCT	Testicular germ cell tumors
THCA	Thyroid carcinoma
THYM	Thymoma
UCEC	Uterine corpus endometrial carcinoma
UCS	Uterine carcinosarcoma
UVM	Uveal melanoma

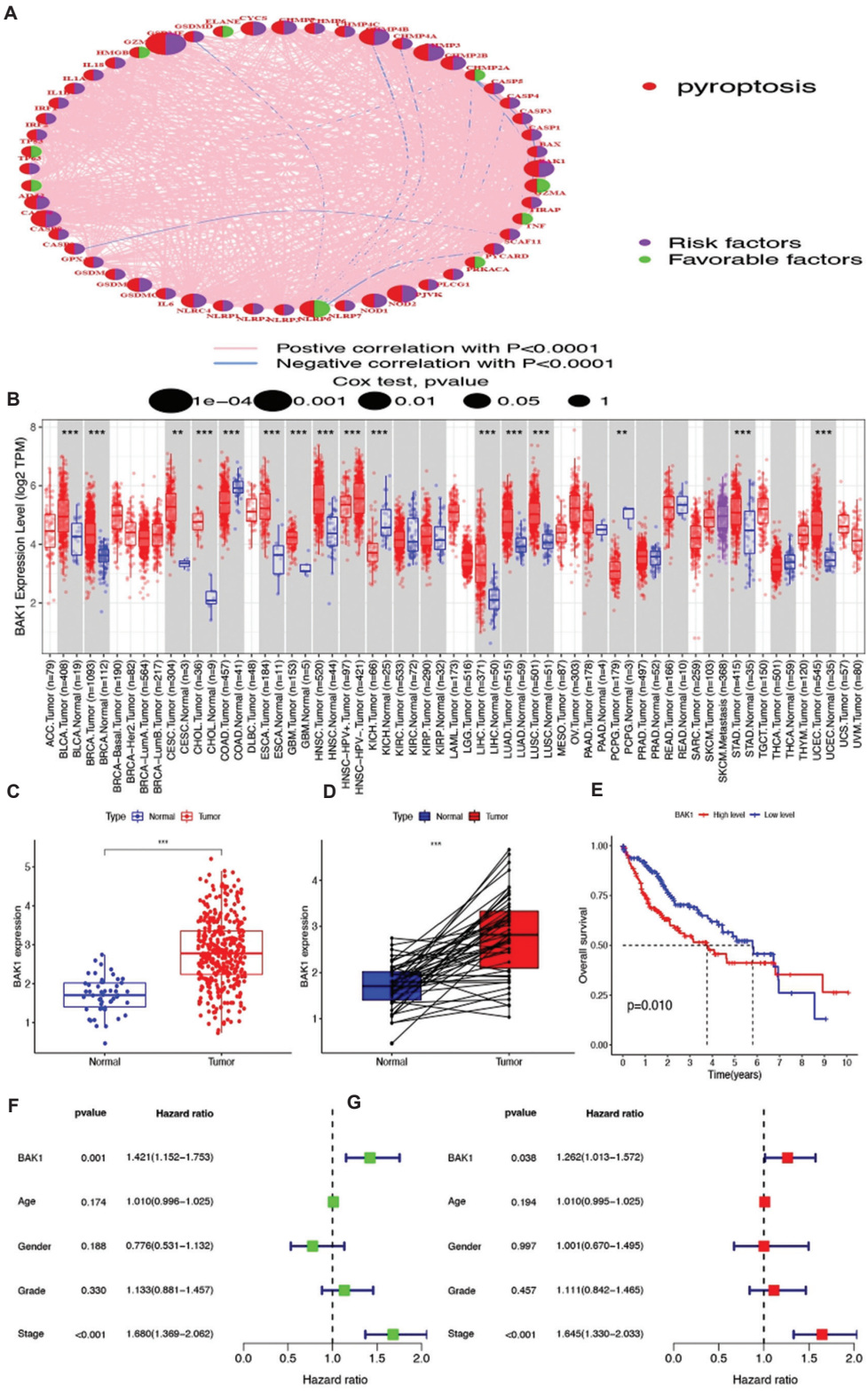


Figure 1. (A) Pyroptosis-related genes interactions in liver cancer. (B) *BAK1* expression levels in several cancer types and matching normal tissues. (C) *BAK1* differential analysis in liver hepatocellular carcinoma (LIHC). (D) Pair-wise differential analysis of *BAK1* in LIHC. (E) *BAK1* survival analyses in LIHC. (F–G) Univariate and multivariate independent prognostic study of *BAK1*. $^{*}P < 0.05$, $^{**}P < 0.01$, $^{***}P < 0.001$.

significantly downregulated in two additional cancer types (colon adenocarcinoma [COAD] and kidney chromophobe [KICH]; all $P < 0.001$). We then looked at how *BAK1* differed between HCC and non-HCC tissues. Figures 1C and D reveal that *BAK1* was expressed at a greater level in HCC tissues and that this level differs considerably from that of non-HCC tissues. We subsequently compared the prognosis of HCC patients with high and low *BAK1* expression; the results revealed that the overall survival rate of HCC patients with high *BAK1* expression was considerably lower than that of patients with low *BAK1* expression (Figure 1E). According to univariate and multivariate independent prognostic analyses (Figures 1F and G), *BAK1* is associated with prognosis and can be a prognostic factor independent of other factors. In univariate Cox regression analysis, the hazard ratio (HR) and 95% confidence interval (CI) were 1.421 and 1.152 – 1.753, respectively ($P = 0.001$); in multivariate Cox regression analysis, the HR was 1.262, and the 95% CI was 1.013 – 1.572 ($P = 0.038$).

3.2. Relationship between BAK1 expression and clinical features

A clinical correlation study was performed to determine if *BAK1* expression differed between clinical groups. *BAK1* exhibited significant differences in gender, tumor grade, tumor stage, and T stage. Figure 2A shows that BAK1 expression does not differ significantly with age. Figure 2B demonstrates that BAK1 expression is significantly higher in female HCC patients than in males. Figure 2C depicts *BAK1* expression levels in various tumor stages, with substantial statistical differences between Stage 1 and Stage 2, as well as Stage 1 and Stage 3. Figure 2D shows a statistically significant difference in BAK1 expression among T1, T2, and T3, but no such difference was seen in the other T stages. The clinical correlation heatmap in Figure 2E shows that the three clinical parameters tumor grade, tumor stage, and T stage have substantial statistical differences between high and low *BAK1* expression groups. Coexpression analysis revealed that *BAK1* is positively regulated by *SMARCD1*, *MFSD10*, *RCC2*, *CDK16*, *PKM*, and *MACROH2A1* but negatively regulated by *GLYATL1*, *ALDH2*, *CDO1*, *DCXR*, and *SLC27A5* (Figure 2F). The diagnostic value of *BAK1* in LIHC was assessed by drawing a receiver operating characteristic (ROC) curve (Figure 2G). We discovered that the area under the ROC curve was 0.694, 0.582, and 0.611 at 1, 3, and 5 years, indicating that this gene may be a good prospective LIHC diagnostic marker.

3.3. Analysis of differential genes and construction of nomogram

All samples were classified into high and low expression groups according to the expression of the target gene *BAK1*, and genes with differences in expression between the high and low expression groups were identified (Figure 3A). The differential genes were found to be involved in neuroactive ligand-receptor interaction, cytokine-cytokine receptor interaction, adenosine 3',5'-cyclic monophosphate (cAMP) signaling pathway, and hematopoietic cell lineage by KEGG enrichment analysis (Figure 3B). We then ran a GSEA, and the results in Figure 3C showed that the four functions HUMORAL IMMUNE RESPONSE MEDIATED BY CIRCULATING IMMUNC, IMMUNOGLOBULIN COMPLEX, IMMUNOGLOBULIN COMPLEX CIRCULATING, and IMMUNOGLOBULIN RECEPTOR BINDING were active in the high BAK1 expression group, and STEROID HYDROXYLASE ACTIVITY is active in the high and low expression group of BAK1. The five pathways FATTY ACID METABOLISM, GLYCINE SERINE AND THREONINE METABOLISM, PEROXISOME, PRIMARY BILE ACID BIOSYNTHESIS, and RETINOL METABOLISM were all active in the low *BAK1* expression group, as shown in Figure 3D. We constructed a nomogram using risk classes and clinical data to predict the 1-, 3-, and 5-year survival in LIHC patients, as shown in Figure 3E. Assuming a patient's composite score is 394, the 1-year survival rate is 0.941, the 3-year survival rate is 0.882, and the 5-year survival rate is 0.839. Correlation plots revealed that the observed and expected rates of survival in LIHC patients at 1, 3, and 5 years were in perfect agreement (Figure 3F).

3.4. Expression of BAK1 and immunity and drug sensitivity

Figure 4A shows a differential study of immune cells, which revealed a statistically significant difference in dendritic cell activation between high and low BAK1 expression groups, suggesting that the activation is favorably regulated by BAK1. Figure 4B, we then examined the relationship between BAK1 and immunological checkpoint-related genes. BAK1 positively regulates CD276, CD86, CD80, TNFRSF8, TNFSF15, LGALS9, TNFRSF18, PDCD1, VTCN1, and HAVCR2, while IDO2 and BAK1 have a skewed relationship. Unfortunately, no significant statistical difference was observed when receiving CTLA-4 and PD-1 treatment regardless of whether BAK1 expression was high or low (Figure 4C and D). Figure 4E and F illustrate the immunohistochemistry (IHC) status of BAK1 in normal and cancerous liver tissue, respectively. Representative IHC photos reveal that BAK1 protein is more abundant in tumors than in non-tumor tissues. We then identified drugs that showed substantial changes in their sensitivity in patients with high and low BAK1 expression. Ninety drugs were discovered. Figure 4G to Figure 4N, Fluorouracil, bosutinib, bleomycin, cyclopamine, and other drugs were

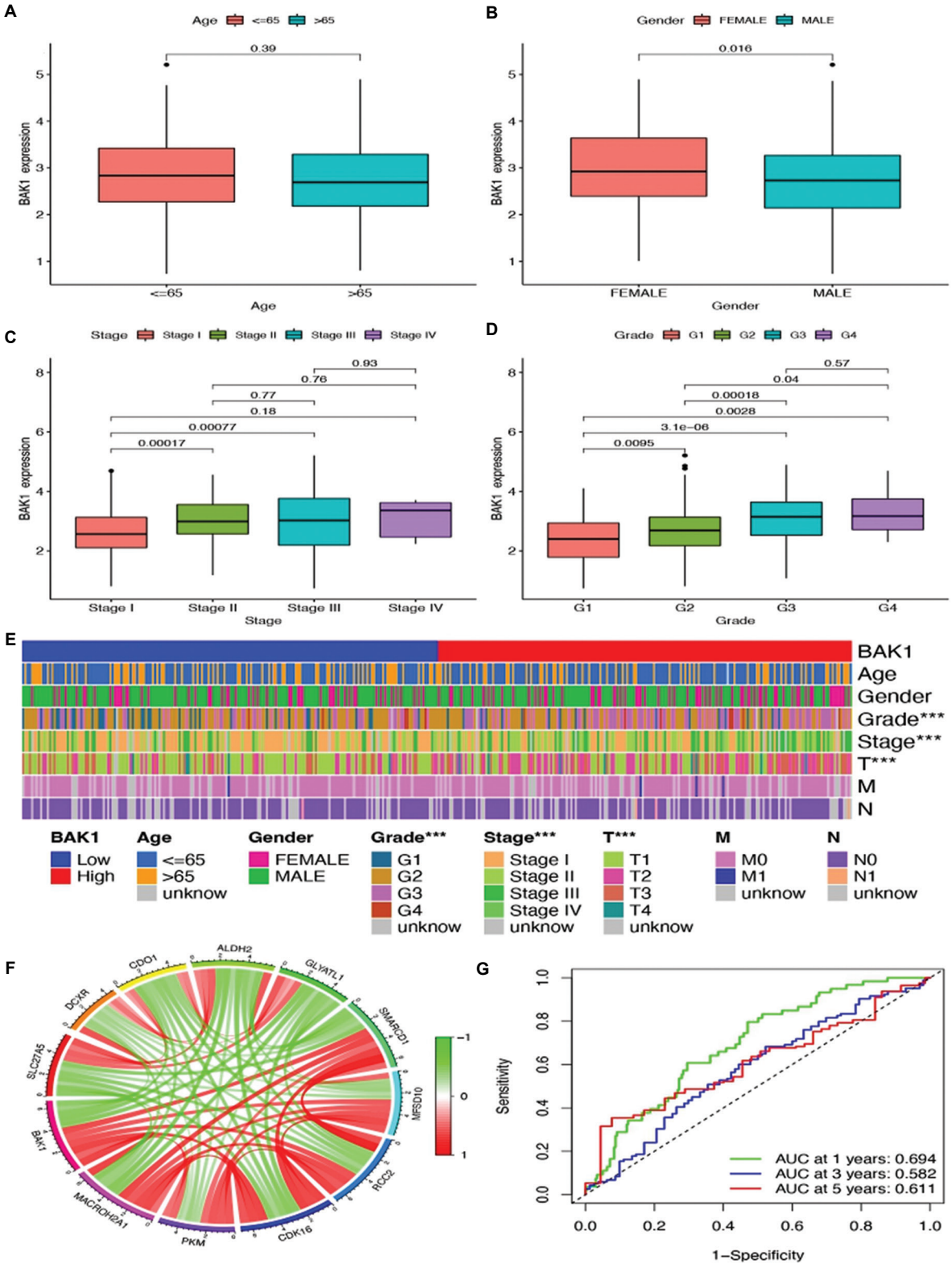


Figure 2. (A–D) *BAK1* correlation analysis by age, gender, tumor grade, and tumor stage. (E) Heatmap of *BAK1* and clinical feature correlations. (F) Genes with *BAK1* coexpression relationship. (G) Receiver operating characteristic (ROC) curves used in GSE 76427 to predict 1-, 3-, and 5-year ROC curves.

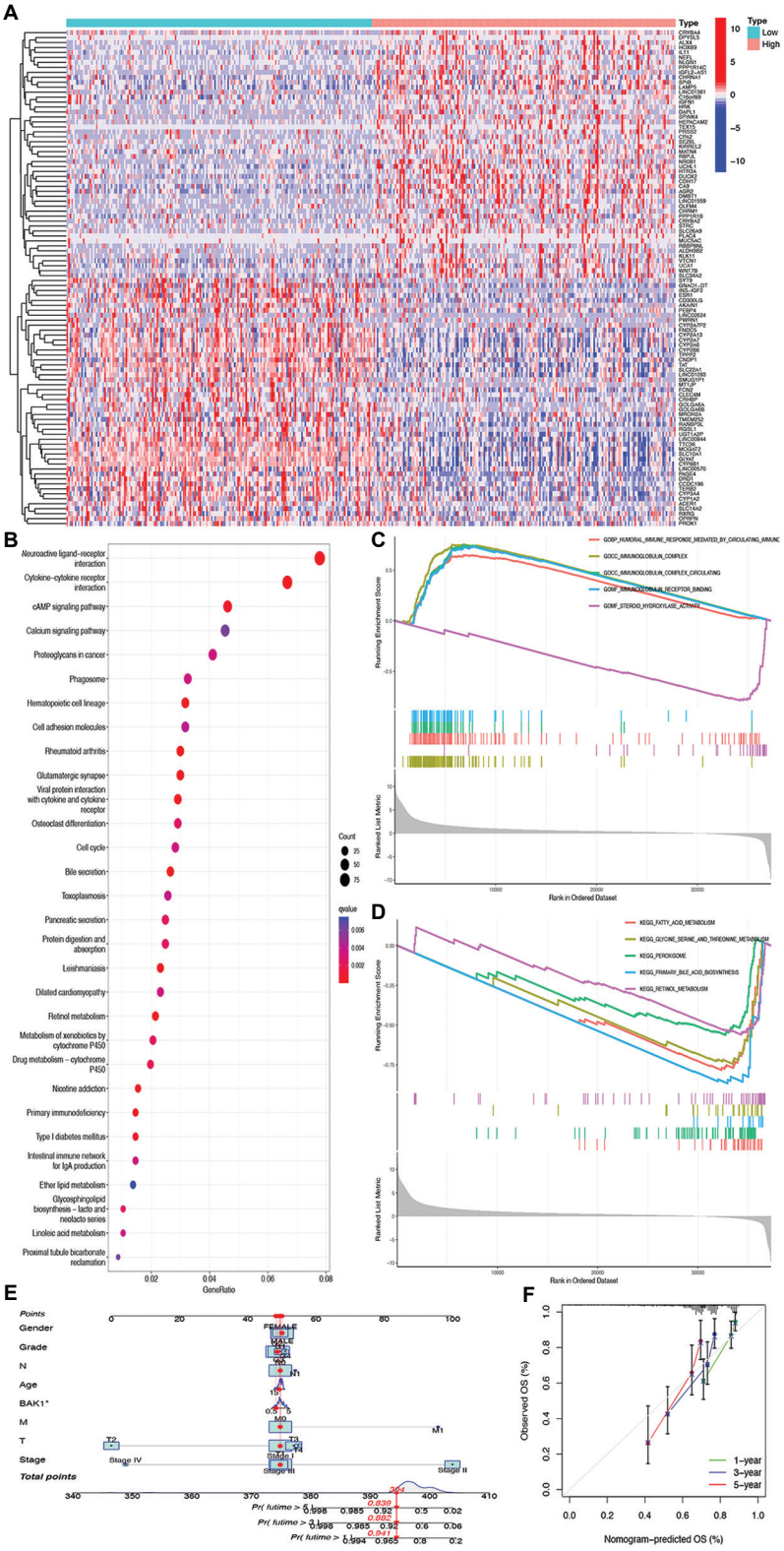


Figure 3. (A) Differential gene analysis in groups with high and low *BAK1* expression. (B) Kyoto Encyclopedia of Genes and Genomes (KEGG) enrichment analysis of differential genes. (C and D) Gene Set Enrichment Analysis (GSEA) of differential genes. (E) A nomogram to predict the 1-, 3-, and 5-year survival in LIHC patients. (F) Calibration curves for the nomogram used in GSE 76427 to predict the 1-, 3-, and 5-year survival.

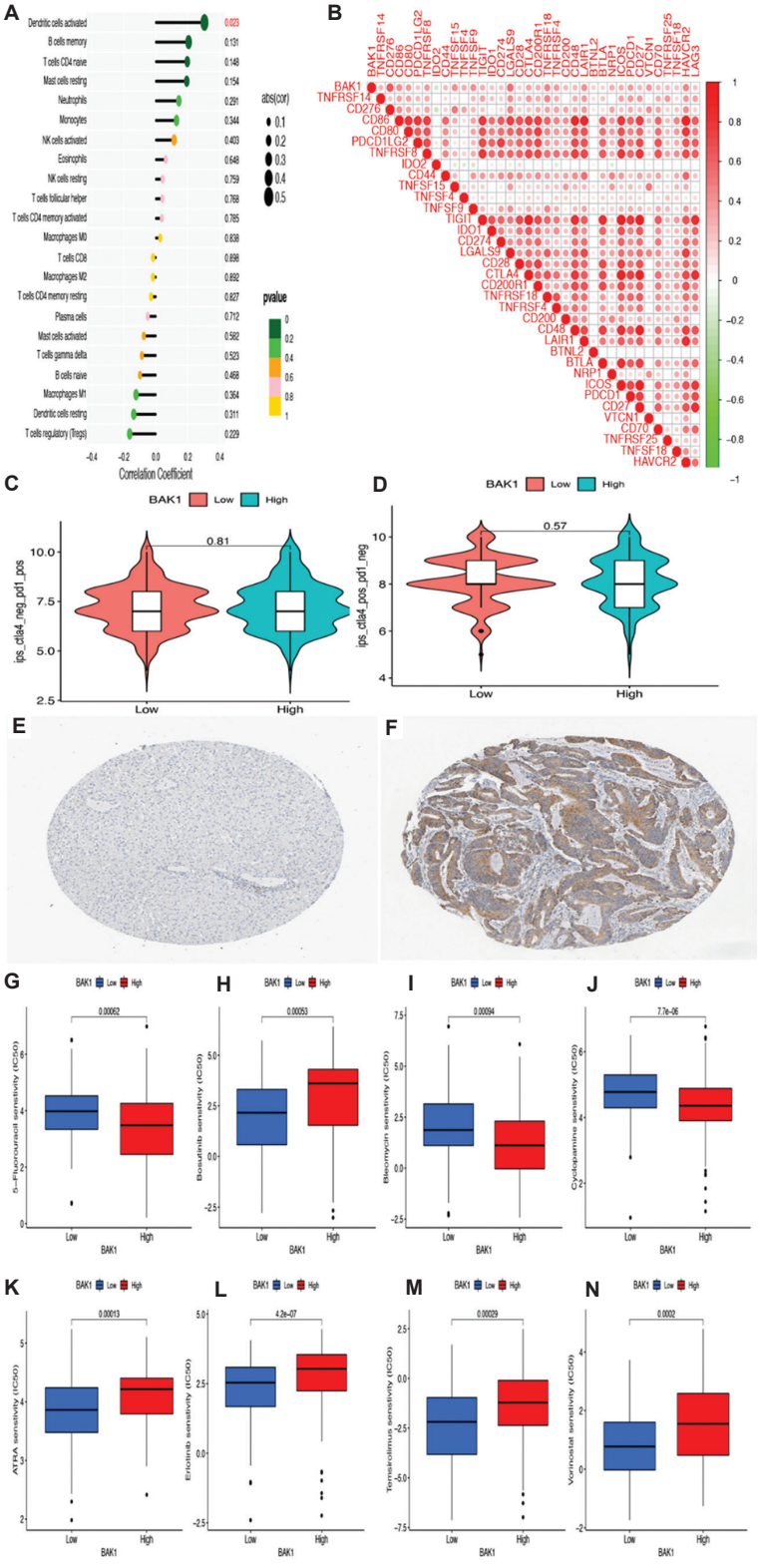


Figure 4. (A) *BAK1* and immune cell correlation diagram. (B) *BAK1* association with immune checkpoint-related genes. (C and D) *BAK1* and immunotherapy correlation study. (E and F) Immunohistochemical pictures of *BAK1* protein in normal and malignant liver tissues. (G–N) Drugs with significant differences in drug sensitivity in high and low *BAK1* expression.

found to be more sensitive to BAK1 expression in patients. Patients with reduced BAK1 expression are more sensitive to all-trans retinoic acid (ATRA), erlotinib, temsirolimus, vorinostat, and other drugs.

4. Discussion

One of the most prevalent primary malignant tumors worldwide is HCC. HCC is often diagnosed at an advanced stage in the majority of patients due to the disease's gradual onset; the early diagnosis of HCC poses a challenge. Certain physiological activities can alter the changes to its indicators due to the poor sensitivity and specificity of early screening, such as serum alpha-fetoprotein (AFP)[13]. Therefore, identifying molecular biomarkers that fully reflect the biological characteristics of liver cancer is a critical link in the early diagnosis and treatment of patients with liver cancer[14,15]. Previous research has looked at the role of pyroptosis-related genes in anti-tumor activity[16]; thus, we set out to investigate the role of pyroptosis-related genes in the prognosis of patients with liver cancer. By examining the predictive value of PRG in 115 HCC patients in the HCC cohort (GSE76427), we discovered that *GSDME*, *CHMP4B*, *CHMP3*, *BAK1*, and *NOD2* are all high-risk genes, which are closely associated with the prognosis of patients. We chose *BAK1* as the target gene for this investigation due to the lack of prior research on the prognosis and immunity of *BAK1* expression in liver cancer. The *BAK1* (BCL2-antagonist/killer1) gene is found on the outer mitochondrial model and belongs to the B-cell lymphoma/leukemia-2 (*BCL2*) gene family[17,18]. The previous research has found *BAK1* to be a prognostic biomarker in women with lung adenocarcinoma[19] as well as a prognostic marker in individuals with colon cancer[20]. It reduces apoptosis and enhances cisplatin resistance in non-small cell lung cancer when combined with cancer-associated fibroblast (CAF)-derived exosomal miR-103a-3p[21]. It has also been shown that *BAK1* is a tumor suppressor gene that regulates cell cycle through microRNA in patients with endometrial cancer[22]. However, there are several studies that have linked BAK1 to HCC diagnosis and prognosis.

The expression of *BAK1* in pan-cancer was investigated using the TIMER database. The expression of *BAK1* was shown to be highly upregulated in 11 cancer types (*i.e.*, BLCA, BRCA, CHOL, ESCA, GBM, HNSC, LIHC, LUAD, LUSC, STAD, and UCEC), but significantly downregulated in two cancer types (i.e., COAD and KICH). We then looked at the differences in *BAK1* expression between HCC and non-HCC tissues; we discovered that *BAK1* was expressed at a greater level in HCC tissues than in non-HCC tissues. The predictive analysis of high and low *BAK1* expression groups revealed that patients with high *BAK1* expression had a considerably poorer overall survival rate than patients with low *BAK1* expression. According to univariate and multivariate independent prognostic analyses, *BAK1* is associated with prognosis and can be independent of other factors. These findings show that *BAK1* could become one of the diagnostic indicators for HCC prognosis. We also constructed a nomogram containing risk classes and clinical characteristics to predict the 1-, 3-, and 5-year survival in LIHC patients, thus making practical application easier. Assuming a patient's comprehensive score is 394, the 1-year survival rate is 0.941, the 3-year survival rate is 0.882, and the 5-year survival rate is 0.839, indicating that it has good prediction ability. The ROC curve was used to assess the diagnostic value of *BAK1* in LIHC, and the area under the ROC curve was 0.694, 0.582, and 0.611 at 1, 3, and 5 years, respectively. According to the findings, the *BAK1* gene may be a good potential LIHC diagnostic marker. Furthermore, we discovered a link between clinical phase features and *BAK1* expression. The findings revealed that *BAK1* expression differed significantly by gender, tumor grade, tumor stage, and T stage, with *BAK1* being more evident in female patients. *BAK1* expression increased with tumor grade in females, and there were significant statistical differences between the other groups except for the expression between G3 and G4. There were statistically significant variations in *BAK1* expression between Stage 1 and Stage 2, as well as Stage 1 and Stage 3. In addition, there was a statistically significant difference in *BAK1* expression among T1, T2, and T3. According to coexpression study, *BAK1* was found to be positively regulated by *SMARCD1*, *MFSD10*, *RCC2*, *CDK16*, *PKM*, and *MACROH2A1*, but negatively regulated by *GLYATL1*, *ALDH2*, *CDO1*, *DCXR*, and *SLC27A5*. The finding of these genes may bring new ideas for multi-biomarker diagnosis in the future.

The differential study of immune cells showed that the difference between dendritic cells activated in groups with high and low *BAK1* expression was statistically significant and exhibited a positive regulatory interaction with *BAK1*. The immune checkpoint-related gene *HAVCR2* is upregulated, while *IDO2* and *BAK1* are downregulated. The finding of these immune checkpoint-related genes may provide specific ideas and directions for the later use of *BAK1* in liver cancer immunological research. Subsequently, we identified drugs that showed substantial changes in sensitivity with high and low *BAK1* expression, of which 90 drugs were discovered. Fluorouracil, bosutinib, bleomycin, cyclopamine, and other drugs were found to be more sensitive to *BAK1* expression. Patients with reduced *BAK1* expression are more sensitive to ATRA, erlotinib, temsirolimus, and other drugs. The discovery of these medications may provide more alternatives for the treatment

of liver cancer in the future, as well as new directions for clinical use and drug development. Our current study, inevitably, has certain limitations. First, our work is based on RNA-sequencing data, derived from public dataset (TCGA), and lacks clinical trials; thus, the predictive ability of all pyroptosis-related prognostic indicators and nomograms needs to be further studied in multicenter clinical trials and prospective investigations. Furthermore, the prognostic role of BAK1 in hepatocellular carcinoma also needs to be further investigated, as does the underlying mechanism.

5. Conclusion

Our data demonstrate that *BAK1* expression is greatly enhanced in LIHC and that high levels of *BAK1* expression are associated with cancer progression and poor prognosis. These findings suggest that *BAK1* may be an oncogene for HCC pathogenesis and progression, as well as a novel prognostic biomarker and potential therapeutic target for HCC.

Acknowledgments

We want to thank TCGA and GEO for the free access to their database.

Funding

This work was supported by the Sanming Project of Medicine in Shenzhen (Grant no. SZSM201612021) and the Research Foundation of Peking University Shenzhen Hospital (Grant no. JCYJ2018002).

Conflict of interest

The authors declare that there are no conflicts of interest.

Author contributions

Conceptualization: Yiyang Chen and Xi Ou
Formal analysis: Yiyang Chen and Yiju Gong
Writing – original draft: Yiyang Chen and Wanbang Zhou
Writing – review & editing: Yiyang Chen

Ethics approval and consent to participate

This study was approved by the Ethics Committee of Peking University Shenzhen Hospital.

Consent for publication

Not applicable.

Availability of data

The datasets presented in this study can be found in online repositories. The names of the repository and accession number(s) can be found in the article.

References

1. Niu LJ, Huang T, Wang L, *et al*., 2022, HBX suppresses PTEN to promote the malignant progression of hepatocellular carcinoma through mi-R155 activation. *Ann Hepatol.*, 27(3): 100688.

2. Liu W, Zheng L, Zhang R, *et al*., 2022, Circ-ZEB1 promotes PIK3CA expression by silencing miR-199a-3p and affects the proliferation and apoptosis of hepatocellular carcinoma. *Mol Cancer*, 21(1): 72.

   https://doi.org/10.1186/s12943-022-01529-5

3. Muhammed A, D'Alessio A, Enica A, *et al*., 2022, Predictive biomarkers of response to immune checkpoint inhibitors in hepatocellular carcinoma. *Expert Rev Mol Diagn*., 22(3): 253–264.

   https://doi.org/10.1080/14737159.2022.2049244

4. Xu X, Mao Y, Tang Y, *et al*., 2022, Classification of hepatocellular carcinoma and intrahepatic cholangiocarcinoma based on radiomic analysis. *Comput Math Methods Med*., 2022: 5334095.

   https://doi.org/10.1155/2022/5334095

5. Niu Z, Xu Y, Li Y, *et al*., 2022, Construction and validation of a novel pyroptosis-related signature to predict prognosis in patients with cutaneous melanoma. *Math Biosci Eng*., 19(1): 688–706.

   https://doi.org/10.3934/mbe.2022031

6. Liu X, Ding S, Liu P, 2021, The roles of gasdermin D in coronavirus infection and evasion. *Front Microbiol*., 12: 784009.

   https://doi.org/10.3389/fmicb.2021.784009

7. Chu Q, Jiang Y, Zhang W, *et al*., 2016, Pyroptosis is involved in the pathogenesis of human hepatocellular carcinoma. *Oncotarget*, 7(51): 84658–84665.

   https://doi.org/10.18632/oncotarget.12384

8. Yan W, Chang Y, Liang X, *et al*., 2012, High-mobility group box 1 activates caspase-1 and promotes hepatocellular carcinoma invasiveness and metastases. *Hepatology*, 55(6): 1863–1875.

   https://doi.org/10.1002/hep.25572

9. Teng JF, Mei QB, Zhou XG, *et al*., 2020, Polyphyllin VI induces Caspase-1-Mediated pyroptosis via the induction of ROS/NF-kappaB/NLRP3/GSDMD signal axis in non-small cell lung cancer. *Cancers* (*Basel*) 12: 193.

   https://doi.org/10.3390/cancers12010193

10. Li H, Zhao XK, Cheng YJ, *et al*., 2019, Gasdermin D-mediated hepatocyte pyroptosis expands inflammatory responses that aggravate acute liver failure by upregulating monocyte chemotactic protein 1/CC chemokine receptor-2 to recruit macrophages. *World J Gastroenterol.*, 25: 6527–6540.

https://doi.org/10.3748/wjg.v25.i44.6527

11. Ye Y, Dai Q, Qi H, 2021, A novel defined pyroptosis-related gene signature for predicting the prognosis of ovarian cancer. *Cell Death Discov*., 7(1): 71.

https://doi.org/10.1038/s41420-021-00451-x

12. Zhang Y, He R, Lei X, *et al*., 2021, A novel pyroptosis-related signature for predicting prognosis and indicating immune microenvironment features in osteosarcoma. *Front Genet*., 12: 780780.

https://doi.org/10.3389/fgene.2021.780780

13. Wang FS, Fan JG, Zhang Z, *et al*., 2014, The global burden of liver disease: The major impact of China. *Hepatology*, 60: 2099–2108.

https://doi.org/10.1002/hep.27406

14. Perisetti A, Goyal H, Yendala R, *et al*., 2022, Sarcopenia in hepatocellular carcinoma: Current knowledge and future directions. *World J Gastroenterol*., 28(4): 432–448.

https://doi.org/10.3748/wjg.v28.i4.432

15. Qu D, Wang Y, Xia Q, *et al*., 2022, Intratumoral microbiome of human primary liver cancer. *Hepatol Commun*., 6(7): 1741–1752.

https://doi.org/10.1002/hep4.1908

16. Tsuchiya K, 2021, Switching from apoptosis to pyroptosis: Gasdermin-elicited inflammation and antitumor immunity. *Int J Mol Sci*., 22(1): 426.

https://doi.org/10.3390/ijms22010426

17. Shimizu S, Narita M, Tsujimoto Y, 1999, Bcl-2 family proteins regulate the release of apoptogenic cytochrome c by the mitochondrial channel VDAC. *Nature*, 399(6735): 483–487.

https://doi.org/10.1038/20959

18. Chittenden T, Harrington EA, O'Connor R, *et al*., 1995, Induction of apoptosis by the Bcl-2 homologue Bak. *Nature*, 374(6524): 733–736.

https://doi.org/10.1038/374733a0

19. Liu Z, Zhang K, Zhao Z, *et al*., 2022, Prognosis-related autophagy genes in female lung adenocarcinoma. *Medicine*, 101(1): e28500.

https://doi.org/10.1097/MD.0000000000028500

20. Feng J, 2022, The p53 pathway related genes predict the prognosis of colon cancer. *Int J Gen Med*., 15: 169–177.

https://doi.org/10.2147/IJGM.S346280

21. Wang H, Huang H, Wang L, *et al*., 2021, Cancer-associated fibroblasts secreted miR-103a-3p suppresses apoptosis and promotes cisplatin resistance in non-small cell lung cancer. *Aging* (*Albany NY*), 13(10): 14456–14468.

https://doi.org/10.18632/aging.103556

22. Witek Ł, Janikowski T, Gabriel I, *et al*., 2021, Analysis of microRNA regulating cell cycle-related tumor suppressor genes in endometrial cancer patients. *Hum Cell*, 34(2): 564–569.

https://doi.org/10.1007/s13577-020-00451-6